J. Fluid Mech. (1986), *vol.* 172, *pp.* 231–258
Printed in Great Britain

On the origin and evolution of streamwise vortical structures in a plane, free shear layer

By J. C. LASHERAS, J. S. CHO AND T. MAXWORTHY
Department of Mechanical Engineering, University of Southern California, Los Angeles, CA 90089-1453, USA

(Received 16 November 1984 and in revised form 24 April 1986)

A plane, isothermal, chemically reacting mixing layer has been experimentally investigated to analyse the origin and the development of three-dimensional streamwise vorticity. The results show that early in its evolution, the plane, free shear layer is composed of counter-rotating pairs of streamwise vortices superimposed upon the spanwise ones. This coherent, streamwise vortical structure was found to be the result of the unstable response of the layer to three-dimensional perturbations in the upstream conditions. Depending on the magnitude and location of the upstream disturbances, the location of the transition to three-dimensionality varied. However, the concentrated streamwise vorticity was always seen to form first on the braids between consecutive spanwise vortices and then to propagate into their cores.

For the low and moderate Reynolds numbers of this study, it was found that the onset of the so-called 'mixing transition' does not necessarily coincide with that of the formation of concentrated streamwise vorticity. These vortices were observed to have a scale, as measured by the size of their cores, somewhat smaller than but comparable with that of the spanwise ones, thus contributing substantially to the entrainment process in the early stages of mixing-layer development.

1. Introduction

Many turbulent reacting flows of practical interest, such as flames, occur in turbulent free-shear layers. The development of suitable models to predict flame characteristics relies heavily on an understanding of the competing mechanisms that control the behaviour of such systems. An understanding of the flow structures that determine the entrainment and mixing of reactants and their coupling with chemical reactions is vital to the development of these models.

In order to elucidate the role of different flow structures in controlling the entrainment and mixing of reactants in a turbulent shear flow, we have undertaken an experimental investigation of a plane, reacting, isothermal, turbulent shear layer. This type of turbulent mixing layer, between two streams of different velocity, plays a key role in the research conducted to improve our understanding of turbulent shear flows.

In a plane mixing layer, large-scale spanwise coherent vortical structures are known to exist. It is believed that they are an essential feature in the development of the turbulent mixing layer, (Brown & Roshko 1971, 1974; Winant & Browand 1974). These two-dimensional structures are a result of the Kelvin–Helmholtz instability caused by the velocity difference. Essentially, this two-dimensional instability can be described as an endless redistribution of vorticity (which the layer initially possesses) in space (Corcos & Sherman 1984). Numerous researchers have

documented the formation and persistence of this highly organized two-dimensional vortical structure (Brown & Roshko 1971, 1974; Rebollo 1973; Winant & Browand 1974; Konrad 1976; Browand & Weidman 1976, among others). Their findings confirm that the spanwise coherent vortical structure is an intrinsic feature of turbulent mixing layers.

In addition to the spanwise coherent vortical structure, it has been found that a plane mixing layer also contains streamwise vortices which are superimposed upon the spanwise ones. For example, Konrad (1976) observed the appearance of streamwise streaks in a plan view of his two-dimensional gas mixing layer. The same type of streak was observed in a mixing layer between two liquid streams by Breidenthal (1978, 1981), which he interpreted as streamwise vortices of alternating signs. These conjectures were confirmed by Bernal's (1981) cross-stream pictures which showed the existence of counter-rotating pairs of vortices superimposed onto the spanwise structures. Jimenez (1983) also observed deformations of the shear layer, which he attributed to the presence of streamwise vortices. Recently, Jimenez, Cogollos & Bernal (1985) have reconstructed a three-dimensional model of a plane, turbulent mixing layer through a digital image-processing technique using the motion pictures of the top and side views of the plane shear layer studied by Bernal in 1981. They found that after the transition to three-dimensionality, streamwise vortices appeared superimposed onto the spanwise structures which still remained largely coherent, thus confirming the earlier results of Konrad (1976) and Breidenthal (1978). Daily & Lundquist (1984) also showed that streamwise streaks appeared in Schlieren photographs of a turbulent, combusting, plane shear layer, concluding that the three-dimensional model postulated by Bernal (1981) and Jimenez *et al.* (1985) is essentially the same in the case of combustion. These experimental studies have shown, without a doubt, the presence of both types of vortical structures (span- and streamwise) in a plane-mixing layer.

The existence of this streamwise, vortical structure has also been predicted theoretically by Corcos (1979), Lin & Corcos (1984), and Corcos & Lin (1984). Corcos & Lin studied the evolution of a roll of weak, alternating vortices with axes parallel to the direction of a uniform, straining flow. Their numerical calculations showed that the streamwise vorticity may evolve into concentrated, round vortices for certain values of the strain and distance between axial vortices. These calculations indicated that streamwise vorticity introduced into the mixing layer would be stretched on the 'braids' between the spanwise vortices under the positive straining existing in that region. This same problem of the dynamics of vortices subjected to stretching has also been analytically studied by Neu (1984). Pierrehumbert & Widnall (1982), through linear stability analysis of a family of coherent, Stuart vortices, suggested that the streamwise vortices could be the result of a 'translative instability'.

Although these theoretical studies provide possible mechanisms for the generation of streamwise vortical structures, the origin and evolution of the three-dimensional vorticity have not yet been determined experimentally.

Wygnanski *et al.* (1979), Browand & Troutt (1980), Breidenthal (1980), Roshko (1980), Oguchi & Inoue (1984) and others have shown that even under the influence of strong external disturbances, the mixing layer is eventually dominated by the presence of the spanwise vortical structure. They concluded that as long as the velocity difference between the two streams is maintained, there is a mechanism that regenerates this spanwise structure. However, their results also showed that the level of initial disturbances has a significant influence on the early stages of development

of the mixing layer. Our findings, presented in this paper, further demonstrate that the intensity of these disturbances determines the location and strength of the concentrated region of streamwise vorticity forming in the flow.

Along with these structural arguments, the role that each of the flow structures (spanwise and streamwise vortices) plays in the processes of entrainment, mixing and chemical reaction that occur in the layer must be further analysed. Brown & Roshko (1974) argued that the entrainment of irrotational fluid into the mixing layers is primarily due to the large spanwise coherent vortical structures. Vortex pairing, an interaction between neighbouring spanwise vortices resulting in their amalgamation to form a larger vortex, has been experimentally observed to be involved in the growth of the shear layer (Winant & Browand 1974). Hernan & Jimenez (1982) have shown that this pairing process is not the only mode of growth of the mixing layer. Their results indicated that most of the entrainment is achieved during the normal life of the large spanwise vortex structures, but not during pairing. Although these varying points of view regarding the governing mechanism of entrainment remain debatable, there appears to be no objection to the idea that these large spanwise vortical structures, through their individual growth and pairing, are responsible for a major portion of the entrainment of irrotational fluid in the mixing layer. However, the quantitative role of the streamwise vortical structure in the entrainment process remains to be analysed.

Our observations, however, show that a significant portion of the overall entrainment may take place due to the streamwise vortices. As a consequence, several relevant questions must then be addressed. (*a*) To what extent do the streamwise vortical structures affect the early stages of development of the mixing layer? (*b*) For how long do these structures maintain a role of importance in the processes of entrainment and mixing? (*c*) Can their formation, location and strength in the mixing layer be controlled?

Dimotakis & Brown (1976) argued that the fluid entrained in the turbulent mixing layer by the large two-dimensional structures remains largely unmixed during the lifetime of the coherent spanwise vortex. Brown & Roshko (1974) also conjectured that very little mixing occurs during the process of entrainment caused by the large spanwise vortices. Similarly, Breidenthal (1978, 1981) concluded that the amount of mixing due to the initial evolution of the large structures is minimal. Koochesfahni (1984) and Masutani & Bowman (1984), through analysis of reacting, turbulent mixing layers, also showed the mixing and reaction caused by the spanwise vortical structures to be minimal. They found that the mixing is localized to a very thin region at the interface between the reactive fluids. After this early stage of mixing associated with the spanwise structure, Konrad (1976) and Breidenthal (1978) observed that the amount of mixing that occurs in the layers increases drastically. They speculated that this so-called 'mixing transition' occurs in the region of the onset of three-dimensional, streamwise vortices, which they associated with their observations of streak patterns. Lin & Corcos (1984), using Neu's analytical solution, evaluated the rate of increase of mixing due to streamwise vortices and concluded that 'it seems probable that at least the onset of mixing transition is caused by the collapse or concentration of streamwise vortices'. Jimenez, Martinez-Val & Rebollo (1979) conjectured that this mixing transition may be associated with the onset of three-dimensionality by reasoning that the enhanced mixing must be due to a sudden increase of the interfacial area resulting from the appearance of the streamwise vortical structures, as suggested by Lin & Corcos' calculations. Postulating that streamwise vortices were indeed present at the 'mixing transition', Bernal (1981)

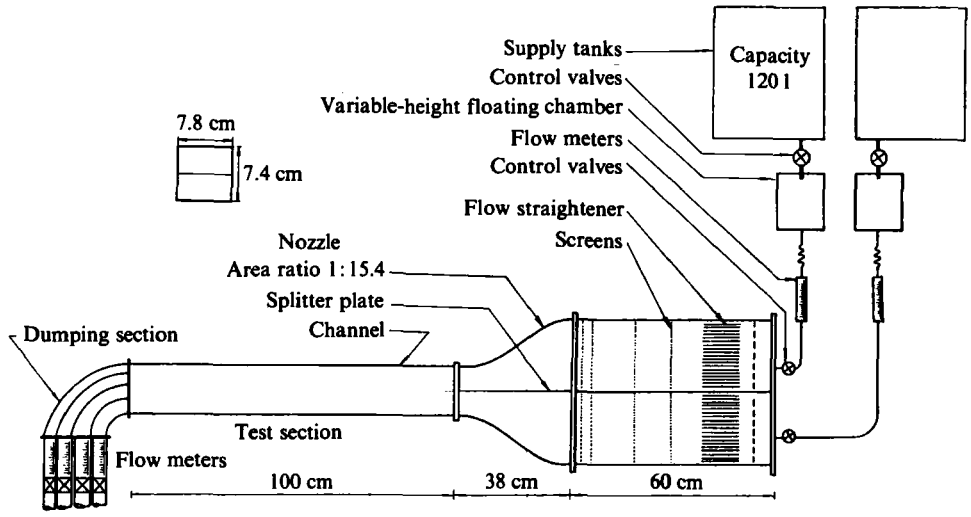

FIGURE 1. Experimental apparatus, channel 1.

concluded that these streamwise vortices cause a gradual mixing of the previously unmixed fluid that has been entrained by the large spanwise structure.

However, questions still remain regarding the initiation and the suddenness of such a 'mixing transition'. Furthermore, its association with the onset of three-dimensionality remains to be studied in more detail. 'Mixing transition' may very well be a result of higher-order instabilities which ultimately break down well-organized spanwise and streamwise vortical structures into smaller-scale ones.

In this paper, we will present a flow-visualization study aimed at analysing the origin and evolution of the three-dimensional, streamwise vortices and their contribution to the entrainment and mixing of irrotational fluid in the mixing layer.

2. Experimental apparatus and diagnosis

2.1. *Experimental apparatus*

Two different low-speed, blow-down water channels were used to produce a turbulent reacting mixing layer between two streams of aqueous solutions. They will hereafter be referred to as channel 1 (small cross-section 7.8 cm high × 7.4 cm wide × 100 cm long) and channel 2 (10 cm high × 10 cm wide × 200 cm long).

In channel 1 (figure 1) the two reactants were fed by gravity from 120 l capacity supply tanks located 2 m above the test section. The main supply tanks were followed by intermediate float chambers to allow control at a constant velocity throughout the testing periods of approximately 10 min. The height of these chambers was variable so that desired flow rates and subsequent flow velocities could be controlled by the head of the intermediate chamber. The mass flow rate in each stream was then controlled by a diaphragm valve and monitored by flow meters. The flow passed through a settling chamber consisting of a distributor, two layers of 60-mesh screens, a layer of honeycomb, and two layers of 40-mesh screens. The latter two layers of screens were removable. The settling chamber was followed by a nozzle. The nozzle's contour was a fifth-order polynomial and was designed after the one constructed by Tan-Atichat (1980). The contraction-area ratio of the nozzle was 15.4:1 to minimize boundary-layer growth and disturbances. The settling chamber and the nozzle were divided symmetrically by a splitter plate. The plate was made

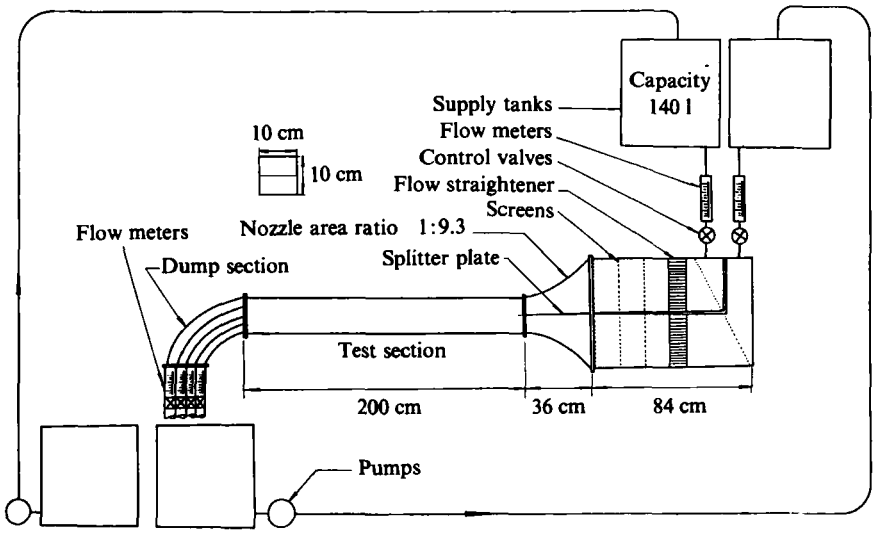

FIGURE 2. Experimental apparatus, channel 2.

of a single, $\frac{1}{16}$ in. thick stainless-steel sheet. A 1 m long, 7.8 cm high × 7.4 cm wide test section followed the nozzle. A dump section was connected to the end of the test section. To minimize the effect of the dumping controls, this section was divided into four separate drains. Each drain was controlled by a separate diaphragm valve and was monitored by an individual flow meter. Under the designated flow conditions, the flow rate passing through each dump section was determined after the velocity profiles had been measured at several downstream stations along the test section.

Channel 2 (figure 2), was a continuously operating channel, designed by K. F. Browand. A complete description of this experimental facility can be found in Winant & Browand (1974). Briefly, this channel was a scaled-up replica of channel 1, although the dimensions and number of screens in the settling chamber were somewhat different. Besides the larger size of the test section (10 × 10 × 200 cm), this facility had the additional advantage of a recirculation system which assured continuous operation at the desired experimental conditions.

2.2. *Experimental techniques*

Velocity measurements

Quantitative measurements of mean velocity profiles, turbulent fluctuations, and mixing-layer growth were obtained by traversing the flow field with a hot-film probe TSI 1210 in the vertical (y) direction, and equally spaced axial positions (x) 5 cm apart (figure 3) between +35 mm and −35 mm from the trailing edge of the splitter plate. The hot-film probe, with a constant-temperature circuit, was calibrated against the known values of the two free-stream velocities. For each set of measurements, the average velocity and the average of the square of the velocity fluctuations were found by evaluating 480 samples for each traverse. The output signal from the probe was recorded on a magnetic-tape recorder (Hewlett-Packard 3950B) and then digitized for digital processing by a Fortran Program using a PDP11 micro computer. The root mean square of the fluctuations is then

$$u'(y) = [(\tfrac{1}{480}) \sum_i (u_i - u(y))^2]^{\frac{1}{2}}.$$

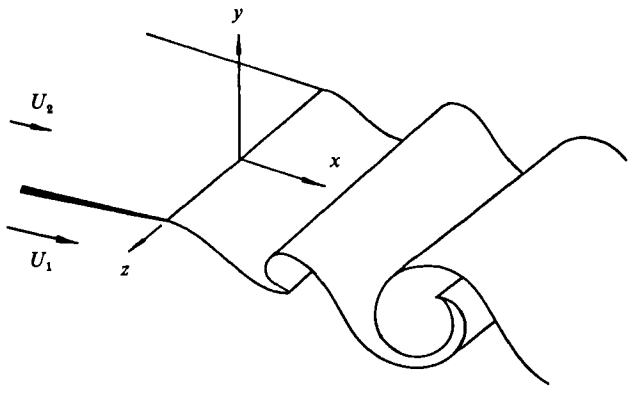

FIGURE 3. Sketch of interface roll-up.

The momentum thickness and vorticity thickness were calculated in the usual way:

$$\theta = \int_{-\infty}^{\infty} \left[1 - \left(2 - \frac{\bar{u} - \bar{U}}{\Delta U}\right)^2\right] \mathrm{d}y, \quad \delta_\omega = \Delta U / \left(\frac{\partial \bar{u}}{\partial y}\right)_{\max}.$$

Flow visualization

Because the primary interest in this study was to investigate the possible cause of three-dimensional, streamwise coherent structures, a flow-visualization technique was used to monitor the position of the interface separating the two fluids and its evolution with time. For this visualization study, a dilute acid-and-base system was used as a second-order, irreversible, one-step reaction process. As pointed out by Breidenthal (1978), although this system is not a perfect, irreversible process, it is an ideal one for a visualization study. Since we were particularly interested in the early stages of the development of the mixing layer, we took advantage of the high-Schmidt-number fluid utilized so that the slow diffusion rates resulted in a very thin (less than 1 mm) region, where the chemical reaction was confined. Thus, the flow-visualization technique gave unique information about the interface location and its changes over time.

The dilute base solution was sodium hydroxide in water with a ph of 11.5. The dilute acid solution was hydrochloric acid with a ph of 6. Both water solutions were prepared with de-ionized water. Water-resolved Cresol Red was added to the acid solution at a rate of 0.04 g l^{-1} as a ph indicator. At the interface, where reaction occurred at a rate much faster than any of the characteristic flow times of our experiment, the reaction product formed became highly visible as the Cresol Red responded to the changes in the ph level (bright red at ph 8.8).

The technique of using an acid/base reaction to visually monitor the mixing layer's characteristics has previously been used in cases of relatively high Reynolds numbers (Breidenthal 1978; Bernal 1979 and many others). However, this flow-visualization technique proved to be a remarkably accurate one for visualizing the interface of the shear layer at low and moderate Reynolds numbers. Here, the problems related to reversibility of the reaction were completely minimized since its use is limited to monitoring the interface during the process of stretching and corrugation under the effect of the large structures. The technique loses its value when higher-order instabilities result in a catastrophic increase in the interfacial area, and the reaction products begin to form in appreciable amounts.

In addition to observing the interface using the Direct Interface Visualization (DIV) technique described above, visualizations of cross-sectional cuts of the layer were performed using Laser Induced Fluorescence (LIF), a technique which was applied initially by Dewey (1976). A water-resolved fluorescent dye, fluorescein, was added to the slow-speed side (base). A plane sheet of light, less than 1 mm thick, was used to excite the fluorescence which was then recorded with conventional still and movie photography. In our experiments we limited the use of this technique to obtain horizontal and vertical cross-cut sections at several X- and Y-positions. In the case of horizontal cross-cuts, pictures were taken with the camera's optical axis perpendicular to the plane of illumination. However, owing to geometrical limitations, the vertical cross-cuts were recorded with pictures taken with the camera's axis at an approximate angle of 15° perpendicular to the visualized plane. The horizontal cuts were therefore those used to quantitatively analyse the different flow structures, while the vertical cross-cuts were used to provide additional qualitative information.

3. Experimental conditions

The primary consideration in selecting the particular values of the free-stream velocities of both the upper and lower flows was the limitation imposed by the flow-visualization technique used in these experiments. Furthermore, the selected values of flow velocities and velocity ratios were within the range of flow conditions used in previous investigations, Winant & Browand (1974), Jimenez *et al.* (1979) and Ho & Huang (1982).

Since the primary goal of this investigation was to determine the origin and evolution of the three-dimensional, organized, streamwise vortical structures in plane, turbulent shear layers, flow conditions were selected that allowed us to visualize a sharp interface and to follow in space and time the evolution of the various structures associated with the overall process. By restricting the range of experimental conditions to cases with low and moderate Reynolds numbers and by limiting the use of flow visualization to the near region of the mixing layer, where the interface is simply being stretched under the effects of the large-scale eddies, the flow-visualization technique is an optimum tool for analysing the origin and evolution of different instabilities in the mixing layer. The accuracy of this technique in observing the precise evolution of the interface can be see in figure 9. However, its usefulness fails when higher-order instabilities result in a catastrophic increase in the interfacial area and a consequential sudden increase in mixing. At this point, problems arise from the reversibility characteristic of the reaction. To accurately measure the amount of reaction that has occurred at a given position, this reversibility should be taken into account. We have limited our study to tracing the interface, thus observing its evolution in space and time.

For these experiments, the velocities of the high- and low-speed free streams were fixed at 6.5 cm/s and 3.5 cm/s respectively. Thus, the ratio of free-stream mean velocities U_2/U_1 was equal to 0.538. Under these conditions, in channel 1 (smaller cross-section) the values of the Reynolds number based on velocity difference $(U_1 - U_2)$ and overall momentum thickness of the layer varied from 36 at 0.25 cm from the trailing edge of the splitter plate to 210 at 15 cm downstream. In channel 2 (larger cross-section) the same conditions produced values of Reynolds number varying from 63 at 0.25 cm from the origin to 270 at 25 cm downstream. Table 1 summarizes the main flow characteristics of the shear layers established in both channels under the above specified free-stream conditions. It should be noticed that

		Channel 1	Channel 2
Free-stream velocity (fast)	U_1	6.5 cm/s	6.5 cm/s
Free-stream velocity (slow)	U_2	3.5 cm/s	3.5 cm/s
Velocity ratio	U_2/U_1	0.54	0.54
Convection velocity	U_c	5.2 cm/s	4.95 cm/s
Momentum thickness		at $x = 0$	at $x = 0$
fast	θ_0	0.585 mm	0.9 mm
slow		0.62 mm	1.1 mm
Total momentum thickness	θ	at $x = 15$ cm	at $x = 25$ cm
		7.0 mm	9.0 mm
Reynolds number	Re_θ		
		at $x = 0$ 36	at $x = 0$ 63
		at $x = 15$ cm 210	at $x = 25$ cm 270
Strouhal number	St	0.047	0.08
Wavelength	λ	2.6 cm	2.5 cm
Spreading rate	$d\delta_\omega/dx$	0.082	0.091
Virtual origin	x_0	−3.0 cm	−3.3 cm
Maximum turbulence level of mixing layer		20%	18%

TABLE 1.

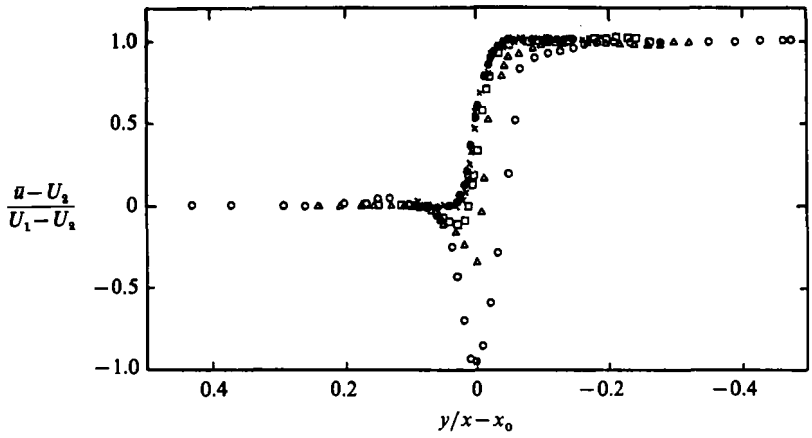

FIGURE 4. Mean velocity profiles, channel 1: ○, $x = 2.3$; △, 6.3; □, 10.3; ×, 15.3; ●, 20.3.

in both cases the boundary layers on the splitter plate in both streams were laminar with momentum thicknesses of 0.58 mm and 0.62 mm for the fast- and slow-speed boundary layers respectively in channel 1, and 0.9 mm and 1.1 mm for the fast- and slow-speed boundary layers in channel 2, (both momentum thicknesses were measured at the geometrical origin of the shear layer.)

Non-dimensional mean-axial-velocity $(\bar{u}-U_2)/(U_1-U_2)$ profiles plotted against non-dimensional vertical distance $y/(x-x_0)$ are presented in figure 4 (channel 1) and figure 5 (channel 2), where x_0 is the virtual origin of the shear layer. The growth of the momentum thickness with distance from the shear-layer origin is shown in figure 6. Notice that for both channels the shear layer is composed of two regions: a laminar region, where the momentum thickness grows as the square root of the downstream distance; and a turbulent region where the shear layer grows linearly with downstream distance. The measured growth rates are 0.032 in channel 1 and 0.038 in channel 2.

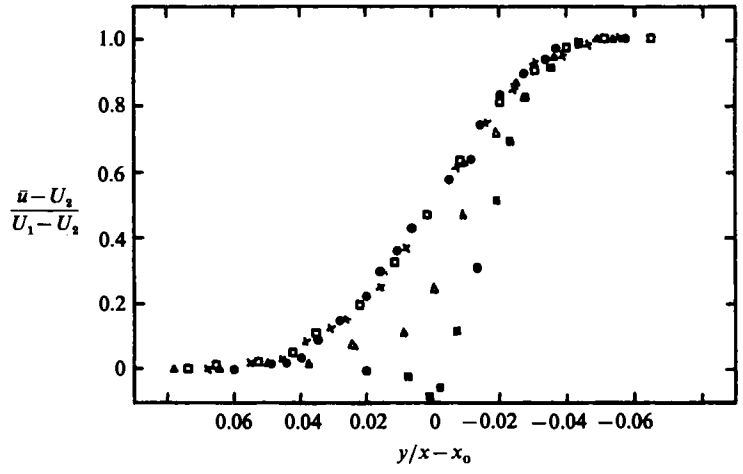

FIGURE 5. Mean velocity profiles, channel 2: ■, $x = 2.3$; ▲, 6.3; □, 12.7; ×, 19.0; ●, 25.0.

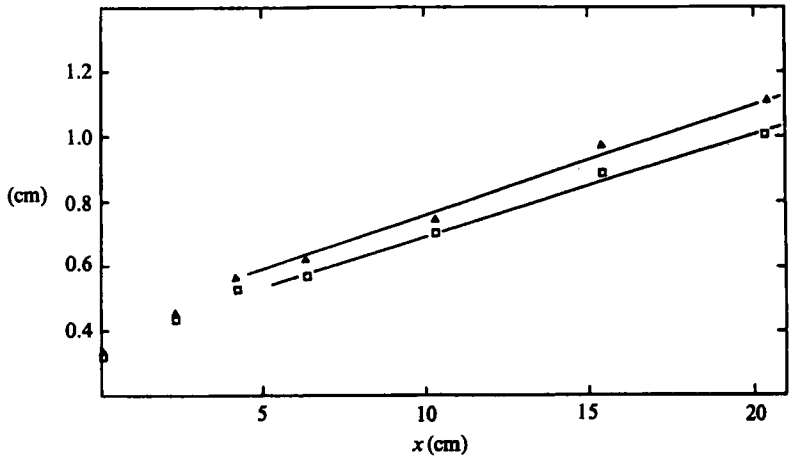

FIGURE 6. Momentum thickness: □, channel 1; △, channel 2.

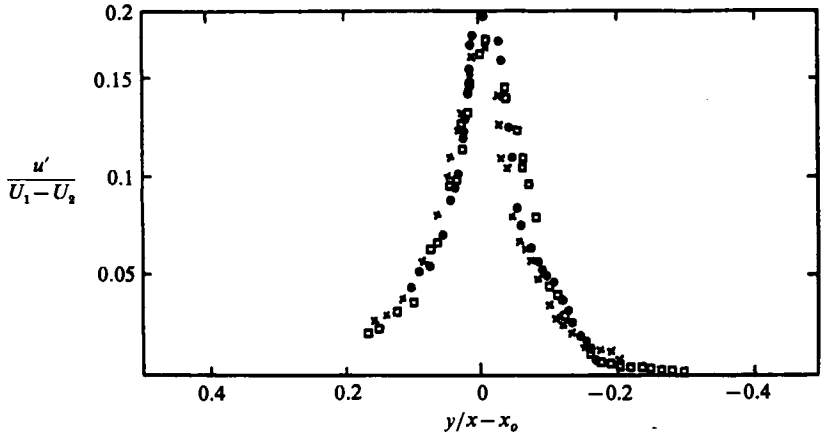

FIGURE 7. Longitudinal velocity fluctuation profiles, channel 1: □, $x = 10.3$; ×, 15.3; ●, 20.3.

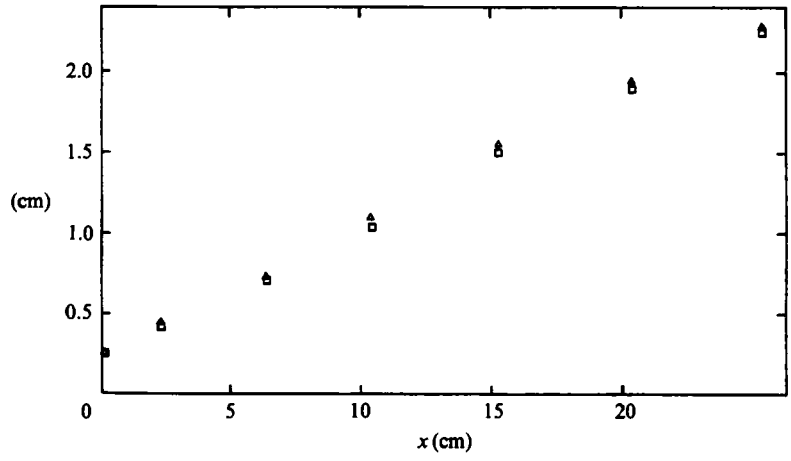

FIGURE 8. Vorticity thickness: □, channel 1; △, channel 2.

Figure 7 shows the distribution of the non-dimensional root-mean-square velocity fluctuation $u'(y)/(U_1-U_2)$. Notice that the distribution measured 10 cm downstream shows a single broad maximum. The maximum disturbance amplitude is 20% of (U_1-U_2) in channel 1 (figure 7) and 18% of (U_1-U_2) in channel 2. These values are in good agreement with those of Jimenez *et al.* (1979). In figure 8, the experimentally determined vorticity thickness of the layer, defined as

$$\delta_\omega = \Delta U/\left(\frac{\partial u}{\partial y}\right)_{\max}$$

is plotted versus the downstream distance x for channels 1 and 2.

The resulting spreading rates are 0.082 and 0.091 for channels 1 and 2 respectively. These values fall within the range of those reported in previous studies by Jimenez *et al.* (0.079), Brown & Roshko (0.081) and Masutani & Bowman (0.071) although, as will be emphasized later, they are very sensitive to the particular experimental conditions.

In order to extend our results to cases of lower Reynolds numbers, we ran a few experiments under the conditions specified in Winan & Browand's (1974) experiments (1.44 cm/s and 4.06 cm/s free-stream velocities for the slow- and fast-speed streams respectively) where the initial Reynolds number was 8 near the origin. In addition, we have also extended our results to cases of moderately high Reynolds numbers by working under the conditions specified by Ho & Huang (1982) (5.0 cm/s and 9.5 cm/s for the slow- and fast-speed free streams respectively).

4. Results of the flow-visualization studies

4.1. *Observations*

The experimental results that follow all correspond to the standard flow conditions of our studies (6.5 cm/s and 3.5 cm/s free-stream flow velocities) unless otherwise specified. Figure 9 shows a top view (*a*) and a side view (*b*) of one of the reacting shear-layer cases investigated in channel 1. It shows that in the initial portion of the layer, where the primary spanwise roll-ups are originated by the Kelvin–Helmholtz instability, reaction is confined to a very thin, diffusion-controlled region at the

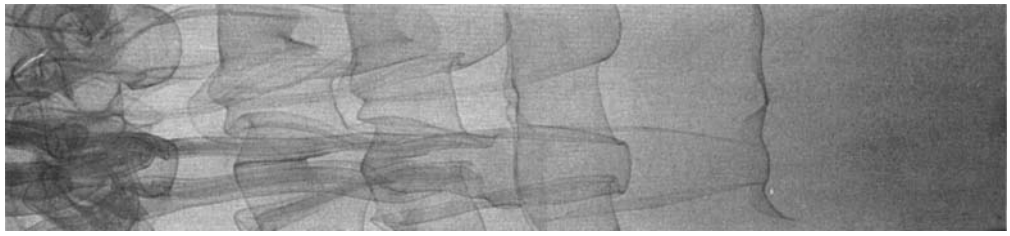

(*a*)

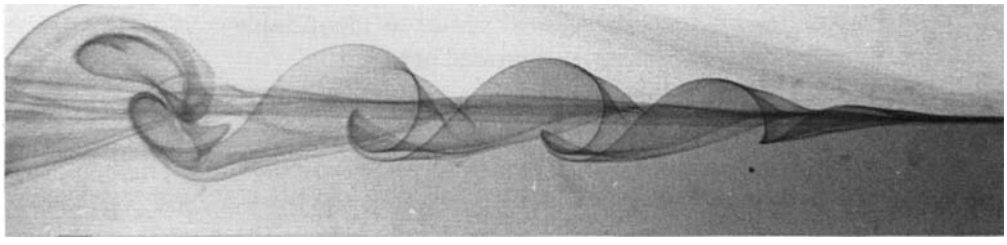

(*b*)

FIGURE 9. (*a*) Top and (*b*) side view of the chemically reacting shear layer in channel 1 ($U_1 = 6.5$ cm/s, $U_2 = 3.5$ cm/s). The flow is from right to left.

interface. For our moderate-Reynolds-number cases owing to the high local strain rate and large Schmidt number, very little reaction is found to occur at the interface. This remains the case so long as the interfacial surface is being stretched by the roll-ups. Further downstream, well-organized, three-dimensional, streamwise vortices can be seen superimposed onto the spanwise vortical structure (see figure 9*a*). We shall show that the transition to this three-dimensional stage is dependent upon the initial level of disturbances existing in both free streams. In this figure, streamwise vortices become apparent as early as the location of the first spanwise vortex. Notice that the streamwise vortical structure remains coherent even after the pairing process has occurred between two spanwise vortices (clearly seen in the side view of figure 9*b*). These experimental results indicate, without a doubt, that even after the transition to three-dimensionality, the reaction is still confined to a very thin but highly distorted interface. Both span- and streamwise vortical structures cause the distortion and enlargement of the interfacial surface where the diffusion-controlled reaction is occurring. Yet at this early stage, they contribute to only a minimal increase in reaction products. Although we have not measured product concentration to identify the location of the mixing transition, our observations suggest that only when higher-order instabilities generate even smaller-scale structures, resulting in a catastrophic increase in the interfacial area, will substantial mixing at the molecular level occur (the so-called 'mixing transition'). These results seem to indicate that the onset of 'mixing transition' does not necessarily coincide with the onset of three-dimensionality, at least not for the low- and moderate-Reynolds-number cases of our studies.

Figure 9 also shows that the scale of the streamwise vortices, as measured by the size of their cores shown by the interface position,† increases as the mixing layer

† The definition of scale that has been applied to characterize both the span- and streamwise vortices is based on the size of the roll-up which can be observed at the interface. Although related, this is not the size of the region of concentration of vorticity.

grows downstream. This is consistent with some of the arguments drawn from spanwise correlation measurements by Jimenez *et al.* (1979) and Bernal (1981) and from some of the streak patterns shown by Brown & Roshko (1974). The important questions that these results pose are:

1. What is the precise location of the transition to three-dimensionality?
2. What are the scales of the three-dimensional vortices in relation to the spanwise coherent structures?
3. To what extent do streamwise vortical structures contribute to the entrainment of irrotational fresh fluid into the layer?
4. How does their presence affect the otherwise two-dimensional spanwise roll-ups?
5. How long do the streamwise vortices persist as identifiable coherent structures superimposed onto the primary spanwise ones?

Transition to three-dimensionality

Experiments performed in both channels have shown that the position where streamwise vortical structures were first observed in the layer varied considerably from run to run. Figure 10 shows five different top views of the mixing layer under our standard operational conditions in channel 1. Clearly shown in these cases is the varying location where concentrated, streamwise vorticity can first be seen. Its location can be noticed as early as just prior to the first spanwise roll-up (cases 4 and 5, figure 10) or as far as the second or third spanwise vortex (case 1, figure 10). Experiments conducted in channel 2 revealed the same randomness concerning the position where well-organized streamwise vortices were initially observed.

It should be noted that although the location of the first manifestation of the streamwise vortices varied, once detected, they were always first found situated on the braids between the spanwise vortices (i.e. in the region of maximum positive strain rate). This can be seen clearly in the different cases presented in figure 10 where the first streamwise 'fold' of the interface is always observed between consecutive, spanwise vortices and then to propagate downstream into their cores. In cases 1 and 2 of figure 10, this first 'fold' is seen between the second and third spanwise vortex. In case 3, it is found between the first and second, while in cases 4 and 5 the 'fold' is initially observed prior to the formation of the first spanwise roll-up. Another interesting observation was the non-symmetrical organization in which these streamwise vortices were often first seen. After propagating downstream and interacting consecutively together, however, they were finally seen organizing into what appeared to be a stable, symmetric configuration consisting of counter-rotating pairs of vortices. During these interactions, we sometimes observed a pairing process among the streamwise vortices of same signs, similar to that observed by Winant & Browand (1974) among the spanwise vortices. These results may help explain the recent findings of Daily & Lundquist (1984) who observed merging of some of the longitudinal 'streaks' found in top-view, Schlieren pictures of a combusting shear layer. However, in all our experiments we noticed that the pairing process terminated after what we call the 'stable configuration' was achieved (i.e. pairs of counter-rotating, streamwise vortices of similar strength). It appears that this type of interaction (pairing) terminates at this stage. We have never been able to observe any other type of pairing interaction once the stable configuration is achieved. Nonetheless, our results do not rule out the possibility that after a spanwise vortex pairing, in which the streamwise vortices redistribute themselves on the braids of the primary structure, some other kinds of interaction among them may exist. The

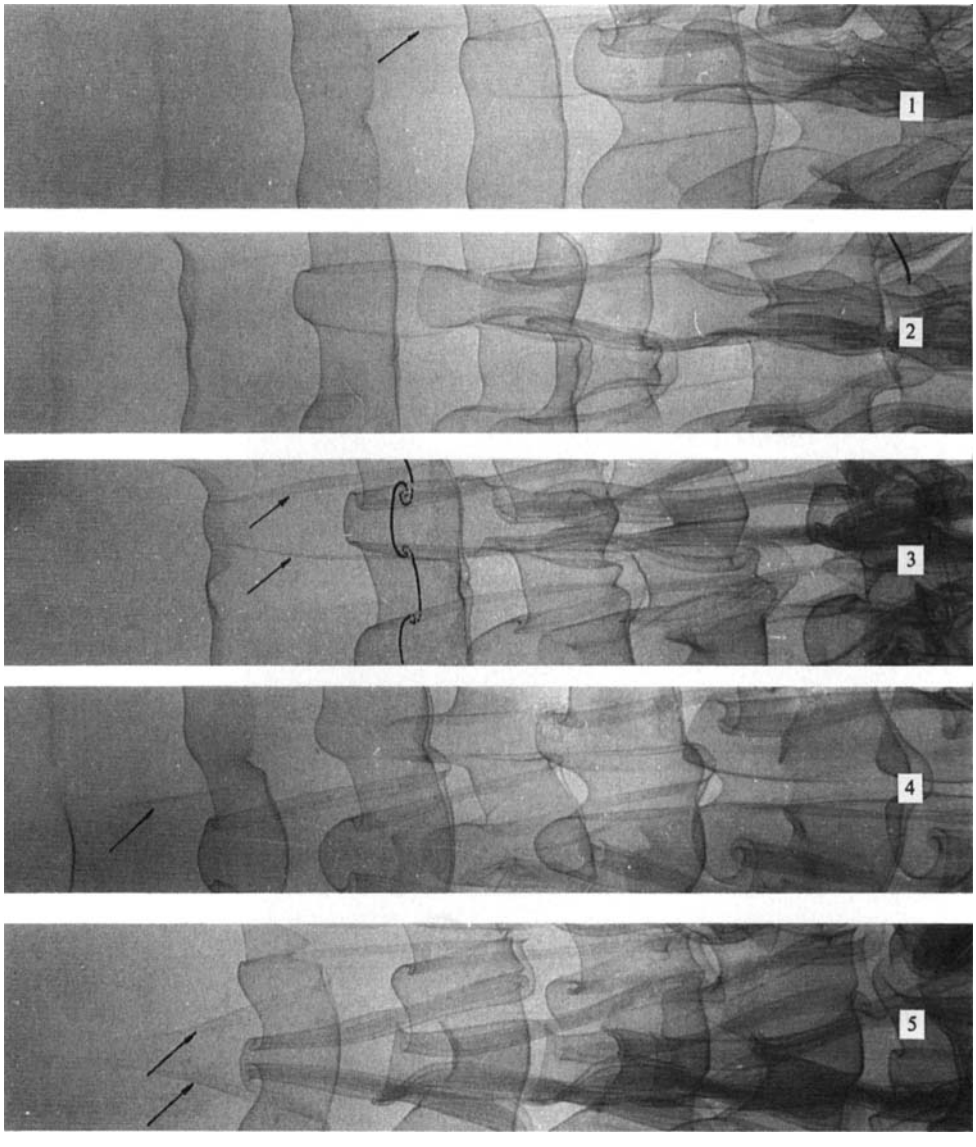

FIGURE 10. Top views showing the organization of five different streamwise vortical structures in the free shear layer ($U_1 = 6.5$ cm/s, $U_2 = 3.5$ cm/s). The flow is from left to right.

limitations of our technique do not allow for clear observations of the structures in the layer at such a late stage.

Scale of the streamwise, vortical structure

In figure 11, several vertical cross-cuts obtained using the LIF technique are presented. These vertical cross-cuts correspond to a location 15 cm downstream of the geometrical origin of the mixing layer (cases A and B), and 20 cm downstream of the origin (cases C and D). All of these experiments were performed in channel 1. Notice that in cases A and B, the streamwise vortices are still organized in a highly non-symmetrical configuration similar to the situation observed in figure 10 (cases

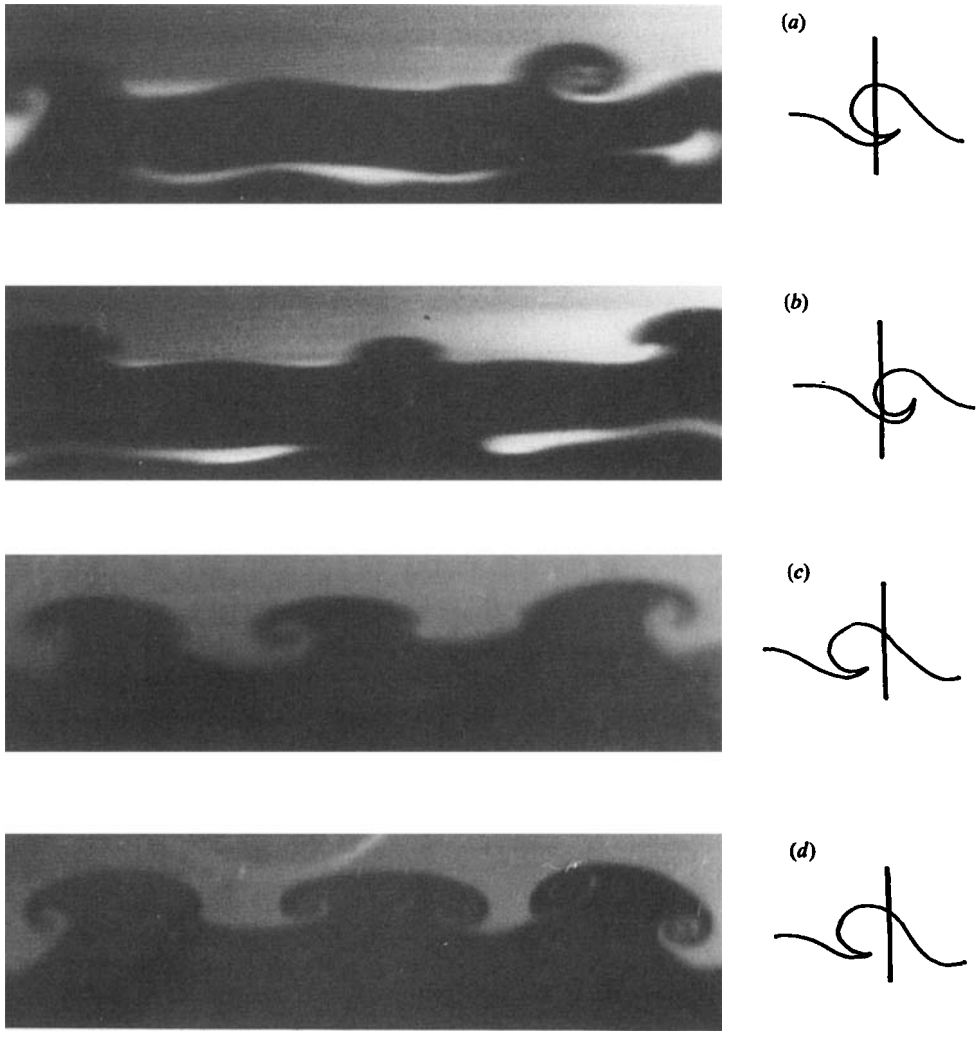

FIGURE 11. Vertical cross-cut using Laser Induced Fluorescence (LIF) at a downstream location of 15 cm (*a*, *b*) and 20 cm (*c*, *d*) from the origin of the free shear layer.

1, 4, or 5) where a non-symmetrical configuration persisted for over 35 cm downstream of the splitter plate. In cases C and D, it can be observed that the streamwise vortices now appear to have organized themselves into a symmetrical configuration consisting of counter-rotating pairs of approximately similar strength. The downstream location where the mixing layer exhibited the streamwise, 'stable' configuration was found to be related to the nature of the initial stages of development of the streamwise structures. On some occasions, such as the ones presented in cases 2 and 3 of figure 10, the 'stable' configuration was observed to be achieved after two or three spanwise wavelengths, while, as mentioned above, in cases 1, 4, and 5 (figure 10) such a configuration was not observed, even 35 cm and more from the trailing edge of the splitter plate.

Consecutive frames of a high-speed (100 f.p.s.) 16 mm film of the vertical cross-cut at a location 20 cm downstream of the origin are shown in figure 12. The figure shows the passage of a spanwise roll-up travelling downstream at a convective velocity

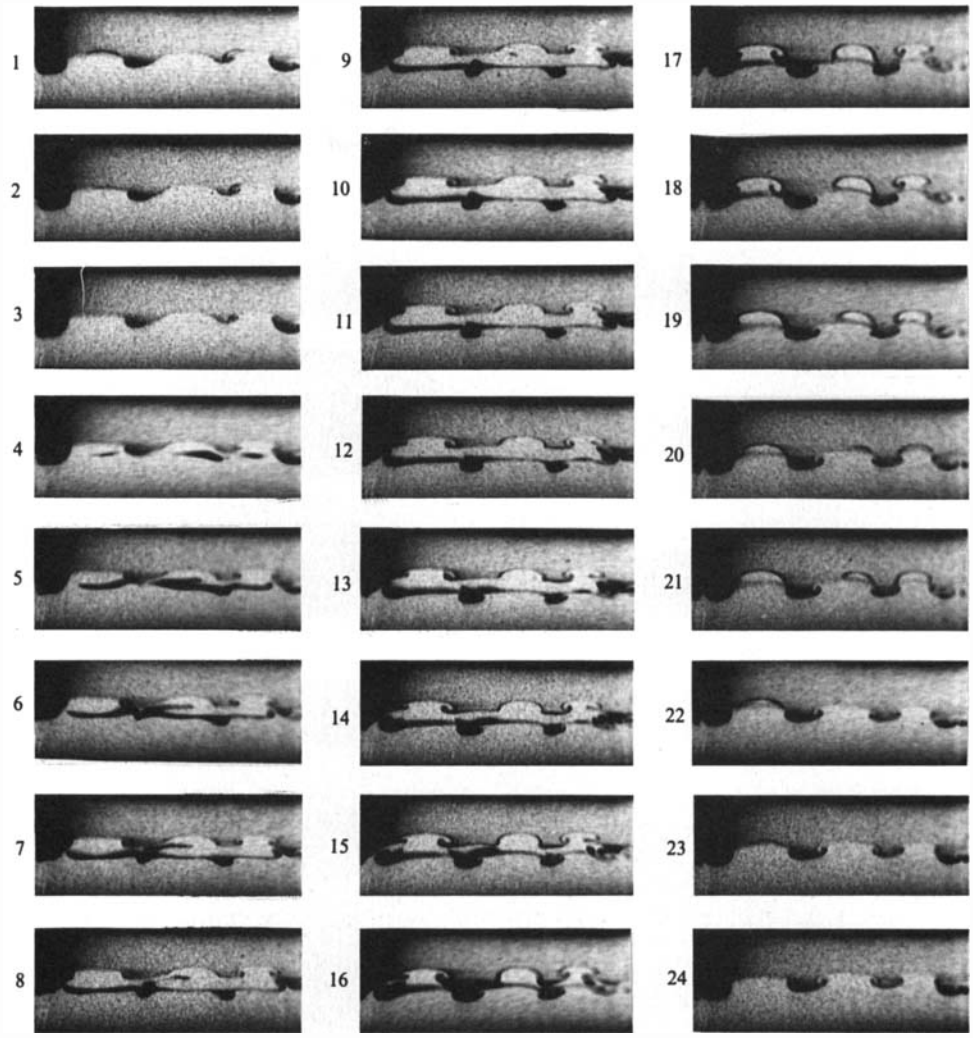

FIGURE 12. Consecutive frames of high-speed 16 mm movie film (100 f.p.s.) of the vertical cross-cut using LIF at 20 cm downstream from the trailing edge of the splitter plate.

approximately equal to the average of the free-stream velocities. Well-organized counter-rotating pairs of streamwise vortices of approximately similar strengths can already be seen to exist on the braids of the primary spanwise structures (sequences 1, 2, 3). Sequences 4–23 show the structure of the cores of the primary spanwise roll-ups. Notice that the streamwise counter-rotating pairs of vortices are observed to exist inside the cores of the spanwise vortices. Sequences 9–14, show this effect remarkably well. After the passage of the spanwise roll-up, the streamwise vortical structures are again shown persisting in the same 'stable' configuration on the following braid (sequences 22, 23, 24).

For our low-Reynolds-number case, the streamwise vortices seem to contribute substantially to the entrainment which occurs in the near region of the mixing layer. This is apparent from their scales which were found to be somewhat smaller, but comparable to those of the spanwise cores (figures 10, 11, and 12). To obtain a clear

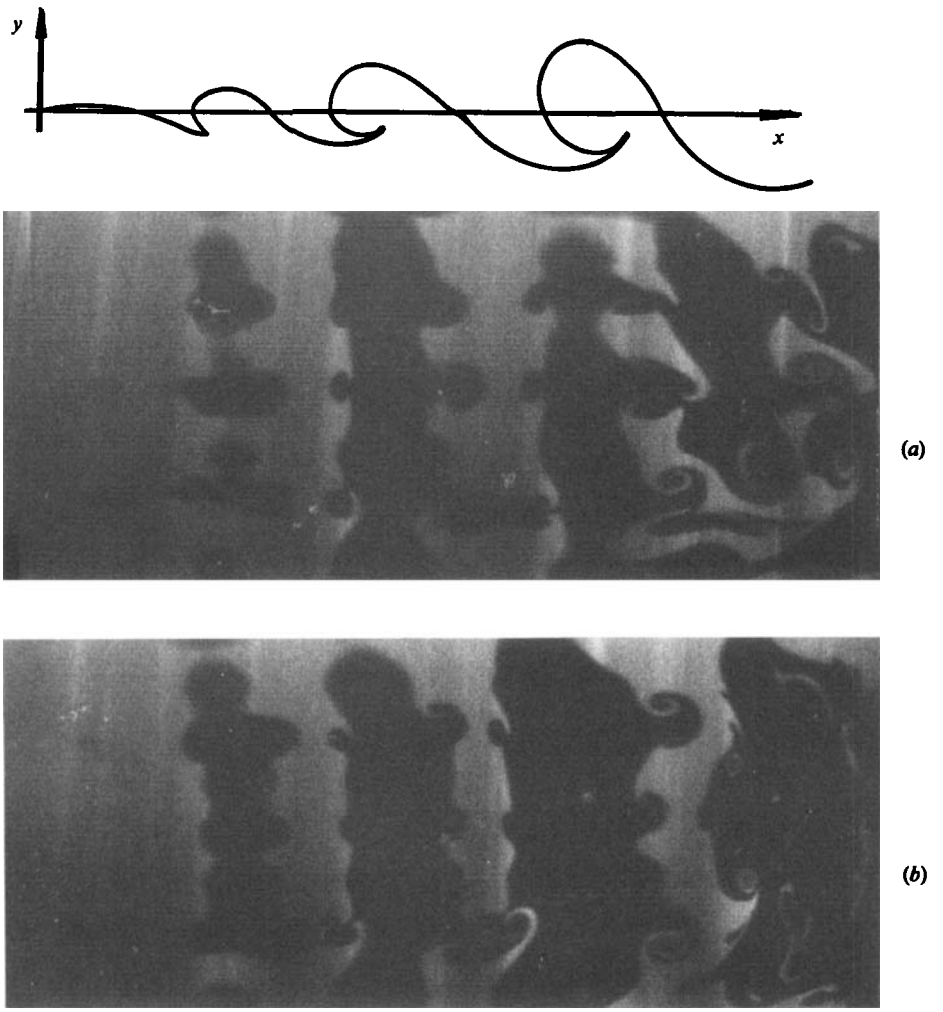

FIGURE 13. Horizontal cross-cut at the plane $y = 0$ using LIF. The flow is from left to right.

indication of the scale of the streamwise vortices, longitudinal cross-cut sections were also recorded using the LIF technique. Two representative cases of longitudinal cuts along the plane $y = 0$ are shown in figure 13. Even from simple, visual analysis of these pictures, it is quite clear that the streamwise vortices account for a large portion of the interfacial surface area. At present we are conducting computerized image-processing of these data. Preliminary results indicate that the effect of the streamwise vortices in stretching and augmenting the interface is increasingly dominant over the effect of the spanwise structures as the three-dimensional vortices propagate downstream.

Effect of three-dimensionality on the evolution of the spanwise structures

Figure 14 summarizes the wide range of behaviour that we have observed under the same experimental conditions. Figure 14 (*a*, *b*) is top and side views respectively, of the shear layer in the case where it has remained almost two-dimensional even

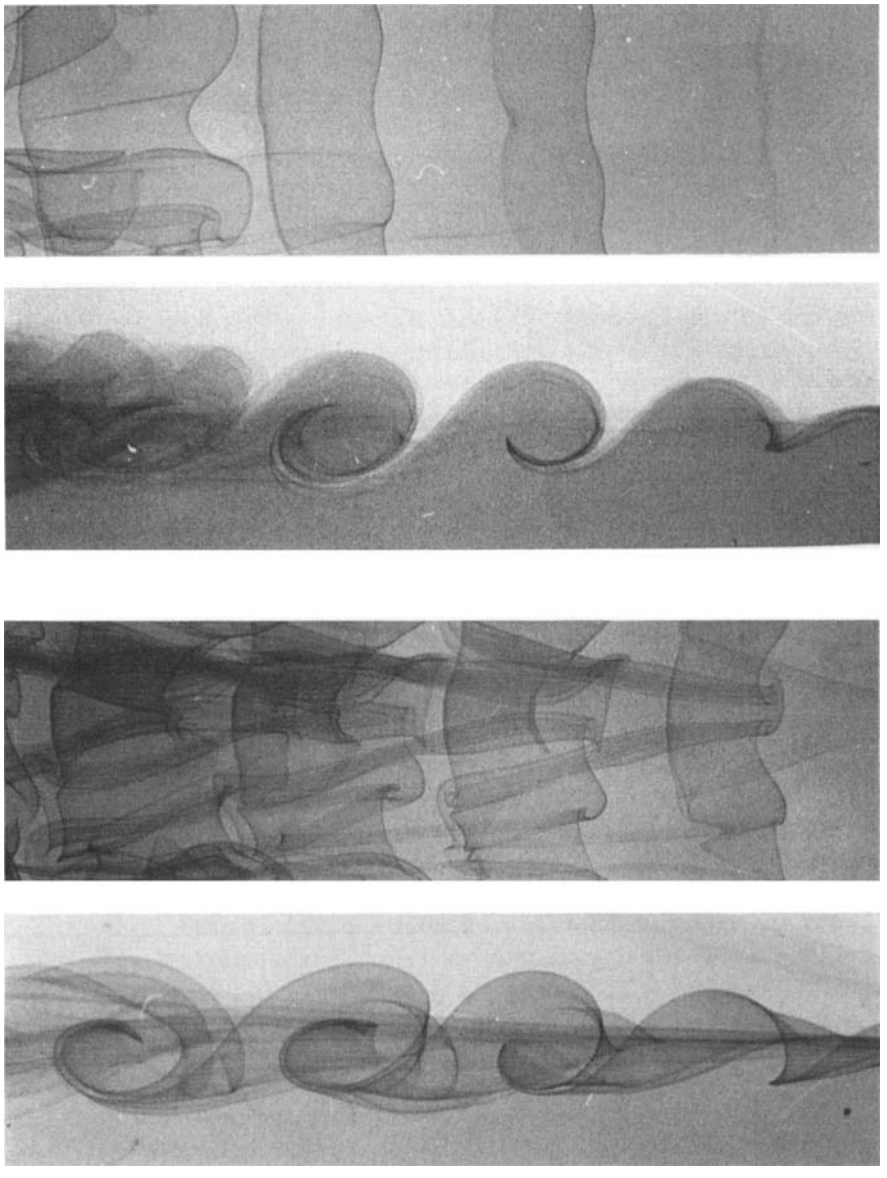

FIGURE 14. Effect of streamwise vortical structures on the spanwise coherent structures. Flow is from right to left.

after three spanwise wavelengths. Figure 14 (*c*, *d*), on the other hand, corresponds to a case where the layer has been three-dimensional from its origin. Notice from the side views that the characteristics of the primary Kelvin–Helmholtz roll-ups are virtually unaffected by the presence of the three-dimensionality. Their frequency, scale and wavelength were found not to be strongly influenced by the three-dimensionality. The reader should be reminded that the side views presented in this paper are not longitudinal cross-cuts of the mixing layer, such as those generated by the injection of dye at one particular y-location, but rather, they show the side view of the full mixing layer, clearly showing its three-dimensional characteristics. As

mentioned before, the scales have been measured by the size of the interfacial roll-ups and the wavelengths as the distance between the centres of the roll-ups.

In addition, the measured spreading rate ($d\delta_\omega/dx$) did not change appreciably from cases 1 to 2. Note that these experimental results indicate that the Strouhal numbers associated with spanwise vortices are unaffected by the presence of streamwise vortical structures. However, from our analysis thus far, it cannot be concluded that the overall vorticity contained in the cores of the spanwise vortices has remained unchanged from case 1 to case 2.

4.2. *The role of upstream disturbances in generating axial vorticity*

From our results thus far, it appears that the mixing layer exhibits, in addition to the primary Kelvin–Helmholtz instability, a secondary instability resulting in the formation of well-organized, streamwise vortical structures. Consequently, we have postulated that the observed changes in the initial stages of development of three-dimensionality could be attributed to the different response of the layer to perturbations of varying location and/or magnitude. In order to analyse the dynamic response of the free shear layer to a localized, small, three-dimensional disturbance, we performed additional experiments in channel 2 under the same flow conditions described above. In this channel, due to the characteristics of its construction, we were able to produce laminar flows in which the level of localized, upstream disturbances in both flows could be minimized. By carefully monitoring the flow, and by removing all the air bubbles from the splitter plate and screens, we were able to produce mixing layers that remained 'almost' two-dimensional after five or six spanwise wavelengths. In this base flow, the response of the shear layer to a localized, three-dimensional disturbance was analysed by introducing a single, small perturbation consisting of a 1.5 mm diameter $\times$ 6.0 mm high vertical cylinder, positioned on the splitter plate at the centre of the channel, 1 cm upstream of the trailing edge.

The top view of the unperturbed case is shown in figure 15, case 1. Notice that the layer is 'almost' two-dimensional, even after the fifth spanwise roll-up. Figure 16 shows the effect of introducing the perturbation in the boundary layer of the fast flow (bottom flow). The flow is from left to right and the trailing edge of the splitter plate can be seen in the far left of the figure. The horseshoe type of vortex shed by the cylinder (Sedney 1973) is convected downstream while being stretched under the effect of the spanwise roll-ups. This vortex pair is noticeable in our flow visualization since it affects the interface immediately. The vortex pair, now oriented in the axial direction, is convected downstream (A in figure 16), but, under the effect of the positive and negative strain created by the large, spanwise vortices, it induces the formation of concentrated regions of streamwise vorticity on either side (B in figure 16). This lateral spreading continues propagating by self-induction (§4.3).

Figure 15, case 2, shows the same flow conditions as in figure 16, but here the perturbation has been placed in the boundary layers of the slow flow (upper flow). Observe that its effect is the same as before; namely the perturbation is being convected downstream, while at the same time, it is spreading laterally, forming regions of alternating strong vorticity which, by the fourth spanwise vortex, already appear organized into the so-called 'stable' configurations consisting of counter-rotating vortices of similar strength. In this case, the vorticity shed from the cylinder is much weaker than in the previous one, and it is much less pronounced than in the flow visualization of figure 16.

When a localized perturbation was introduced into a base flow containing small,

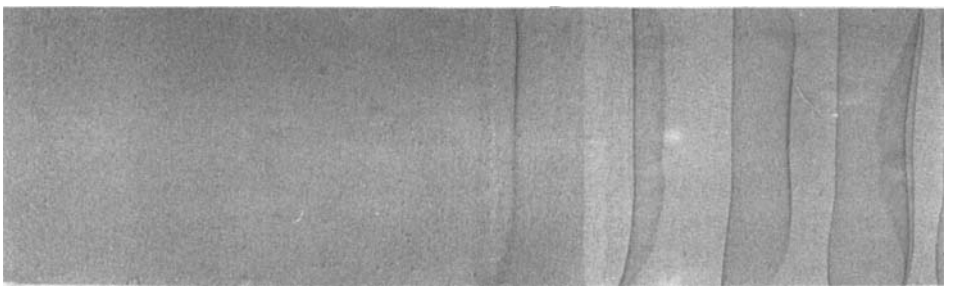

case 1

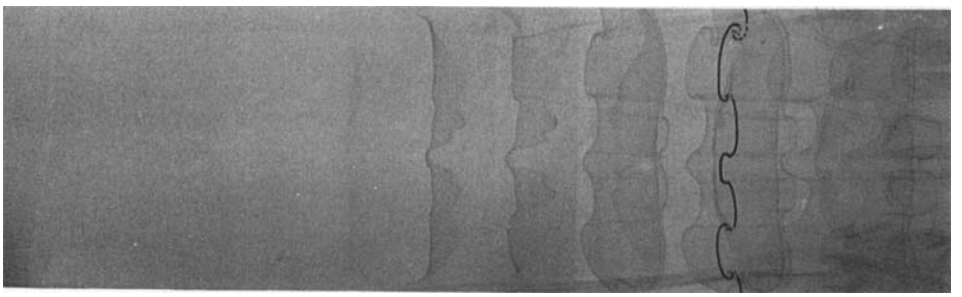

case 2

FIGURE 15. case 1: top view of the shear layer ($U = 6.5$ cm/s and $U = 3.5$ cm/s) in channel 2 in the absence of upstream disturbances, showing an 'almost' two-dimensional structure down to the fifth spanwise roll-up. Case 2: effect of a small three-dimensional perturbation introduced in the same layer as in case 1, at a location 1 cm upstream of the trailing edge of the splitter plate in the boundary layer of the slow flow.

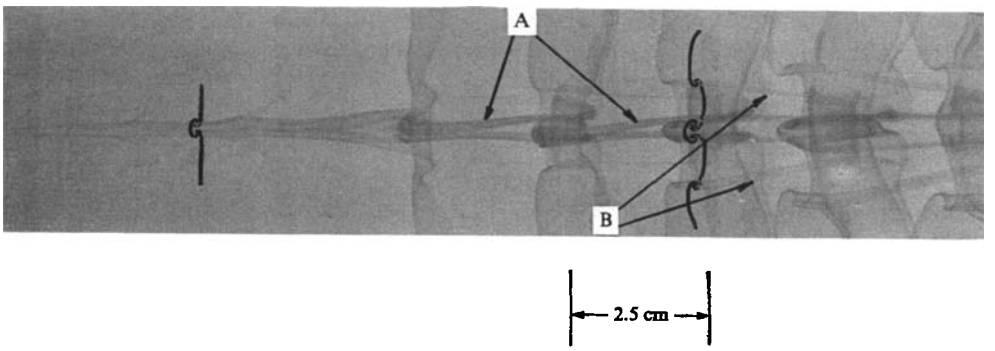

FIGURE 16. Top view of the shear layer ($U = 6.5$ cm/s and $U = 3.5$ cm/s) showing the propagation of the localized small disturbance introduced 1 cm upstream of the trailing edge of the splitter plate in the boundary layer of the fast flow. The trailing edge of the splitter plate is shown in the far left. The flow is from left to right.

random disturbances, either in the free streams or in the boundary layers, the result was even more dramatic. Figure 17 shows three runs of a case where the base flow contains small, random disturbances and where, in addition, a localized perturbation has been introduced into the boundary layer of the fast flow. The position where the streamwise vorticity is first detected is obviously when the perturbation was introduced (the horseshoe vortex shed by the cylinder is indicated by an arrow in

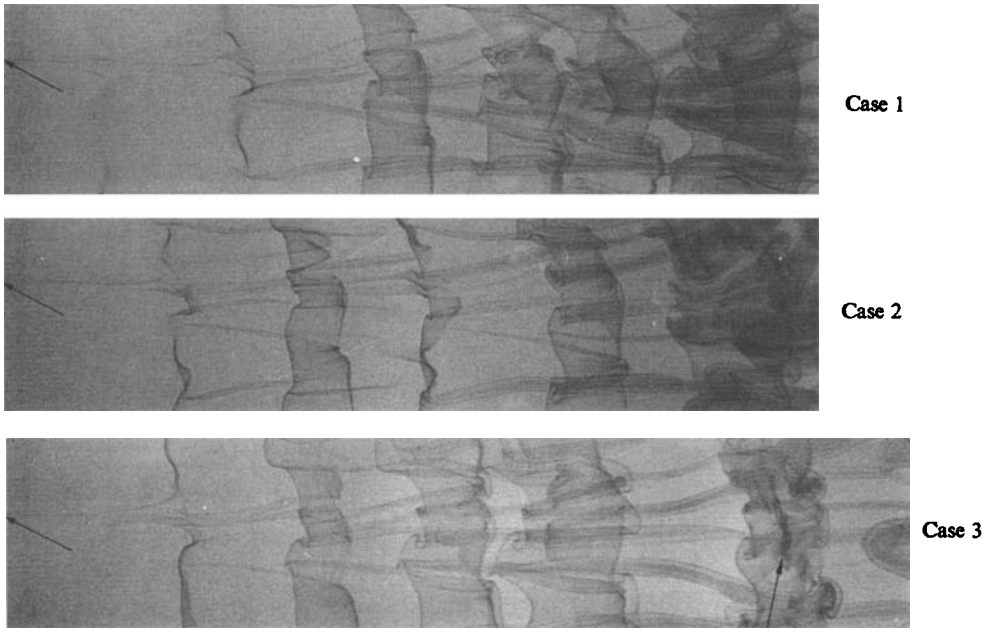

FIGURE 17. Effect of a perturbation, introduced 1 cm upstream of the trailing edge of the splitter plate in the boundary layer of the slow flow, in a flow containing random, small upstream disturbances.

each of the pictures). Observe that here the perturbation has also resulted in concentrated regions of streamwise vorticity which are convected downstream while propagating laterally. However, the streamwise vortices induced sideways vary in location and number from run to run. Notice that in case 3 of figure 17, the perturbation has induced the formation of other streamwise vortices which increase in number as they move downstream.†

Also, observe that they persist superimposed onto the primary structure even after a pairing has occurred between two consecutive spanwise vortices (far right of figure 17, case 3). After observing such a strong response of the shear layer to localized perturbations introduced in the boundary layers of either the fast or the slow flows, it became obvious that the observed differences in the location of the onset of three-dimensionality were created by uncontrolled upstream perturbations existing in our experimental channel. These consisted of small bubbles which attached to either the splitter plate or the screens and caused perturbations in the boundary layers or free streams, thus triggering the unstable behaviour of the layer.

We conducted additional experiments under the conditions specified above by changing either the location, the size, or the shape of the perturbation. The vertical cylinder was replaced by half-spheres 2 mm in diameter or by differently shaped, small, vortex generators. We repeatedly found the same qualitative behaviour, namely the unstable response of the shear layer to the small, three-dimensional disturbances. By placing the perturbations in the boundary layers of either flow, we were able to accelerate the transition to three-dimensionality (a disturbance existing

† The weak, diffused vorticity that may exist in the flow does not show in the pictures. This flow visualization shows only the regions where vorticity is concentrated in a vortex tube.

in a free stream is injected much farther downstream, thus, its effect – transition to three-dimensionality – occurs farther downstream). Furthermore, we found that the number of streamwise vortical structures was related to the magnitude and location of the upstream disturbances, and was probably controlled by the interaction mechanism between structures created by separate perturbations. These results are in agreement with the observation reported by Jimenez (1983) who, from spanwise variations in the velocity measurements, expressed his suspicion that some of the streamwise vortical structures could have originated from small non-uniformities in the screen (free stream) or by small obstacles in the boundary layers on the splitter plate. He found that the position and number of streamwise vortices in the layer was changed by rotating the screens in the settling chamber.

Through the interaction of the large, spanwise vortices with the vertical sidewalls, we also observed the generation of axial vorticity, which spreads laterally into the channel in a fashion similar to that observed in the spreading of the localized perturbation (Lasheras & Maxworthy 1985). In the cases where we were able to impose only one localized perturbation in an otherwise almost two-dimensional layer (at least down to the fifth or sixth spanwise roll-up) we found that the number of streamwise vortices that eventually organized into the so-called 'stable' structure, was determined by the interaction mechanism between the vortices induced by the perturbation and the ones generated at the sidewalls. In the cases where the layer was exposed to more than one localized perturbation, the interacting effect between flow structures induced by each of them determined the number and the strength of the streamwise vortices that eventually constituted the 'stable' configuration. An analysis of the dynamic response of the free shear layer to periodic spanwise disturbances (in the absence of the sidewalls' effect) and the interaction between the flow structures induced by them will be presented in detail in a subsequent paper (Lasheras & Choi 1986).

4.3. *Mechanisms of axial vorticity production*

Under the primary Kelvin–Helmholtz instability, the spanwise vorticity that the layer initially possesses is redistributed in space into regions of concentrated strong vorticity (cores) and relatively weak vorticity (braids). The interface of the braids is under the strong positive strain rate caused by the nearby cores. The combined effects of the large positive strain rate and the vertical shear on the braids can result in an unstable response of spanwise vortex lines to small three-dimensional perturbations.

The results presented above (§4.2) show that three-dimensional vorticity injected into the layer is stretched by Corcos' mechanism (1979) collapsing into regions of concentrated, strong streamwise vorticity. However, the observed lateral spreading of this disturbance, which leads to the formation of streamwise vortices sideways of the perturbation, suggests a possible reorientation of the existing vorticity in the layer from the spanwise direction into the direction of the strain field. This may occur in a fashion similar to that shown in Pierrehumbert & Widnall's linear instability analysis (1982), i.e. their 'translative instability'.

In the following, we shall propose a possible mechanism for developing the observed, 'wave-like', lateral propagation of the localized disturbance. Any small three-dimensional perturbation (with either or both axial and vertical vorticity) affecting the interface at a location of positive strain will result in a small deformation (kink) of the axis of the primary spanwise vorticity, as shown in figure 18(*a*). The positive strain rate will then stretch the originally small kink in the streamwise

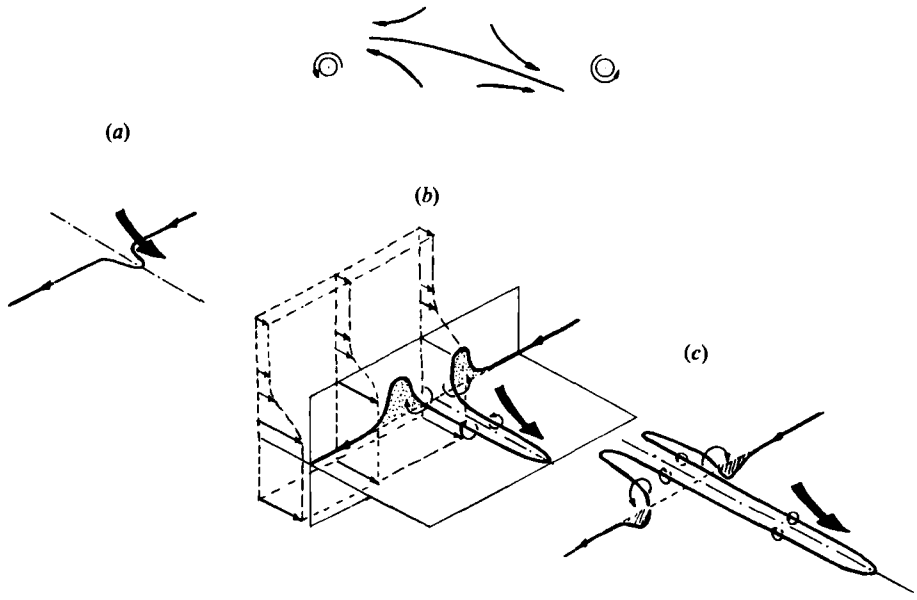

FIGURE 18. Mechanism of axial vorticity generation.

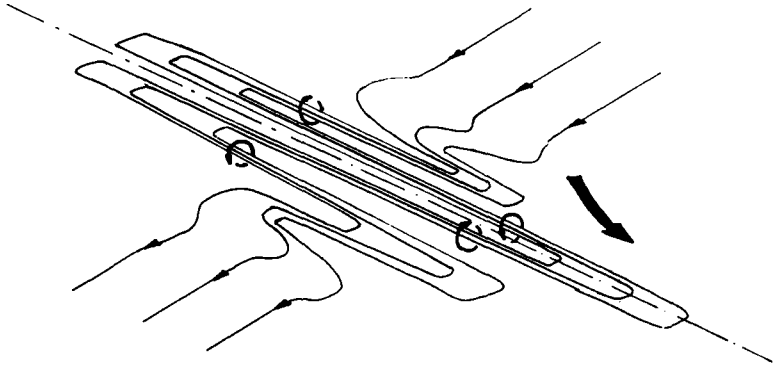

FIGURE 19. Concentration process involved in the formation of streamwise vortices from initially spanwise-oriented vorticity.

direction (figure 18*b*) producing a pair of counter-rotating streamwise vortices. Under their influence, the vortex lines will be further lifted upward at the sides of the evolving longitudinal vortices. The vertical shear and/or strain will then orient the vortex axis in the axial direction where the positive strain will continue to stretch the pair of vortices (figure 18*c*). Provided that the positive strain and the vertical shear are maintained, this effect will continue to magnify as well as to propagate sideways.

This nonlinear mechanism proposed above could, therefore, be responsible for the redistribution of the weak spanwise vorticity still existing on the regions of positive strain (braids) to form stronger streamwise vortices. This effect is presented schematically in figure 19. Recently, Ashurst & Meiburg (1985) have produced numerical calculations of a mixing layer via vortex dynamics where they show the nonlinear development of the vorticity between two consecutive spanwise vortices. In partic-

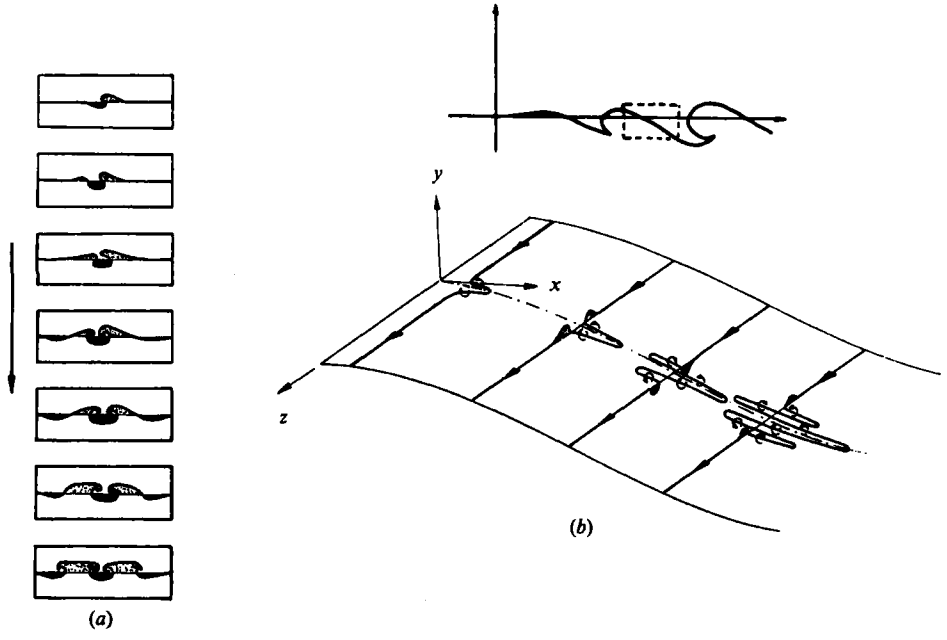

FIGURE 20. Sketch of the development of streamwise vortical structures from the unstable response to a small, three-dimensional perturbation.

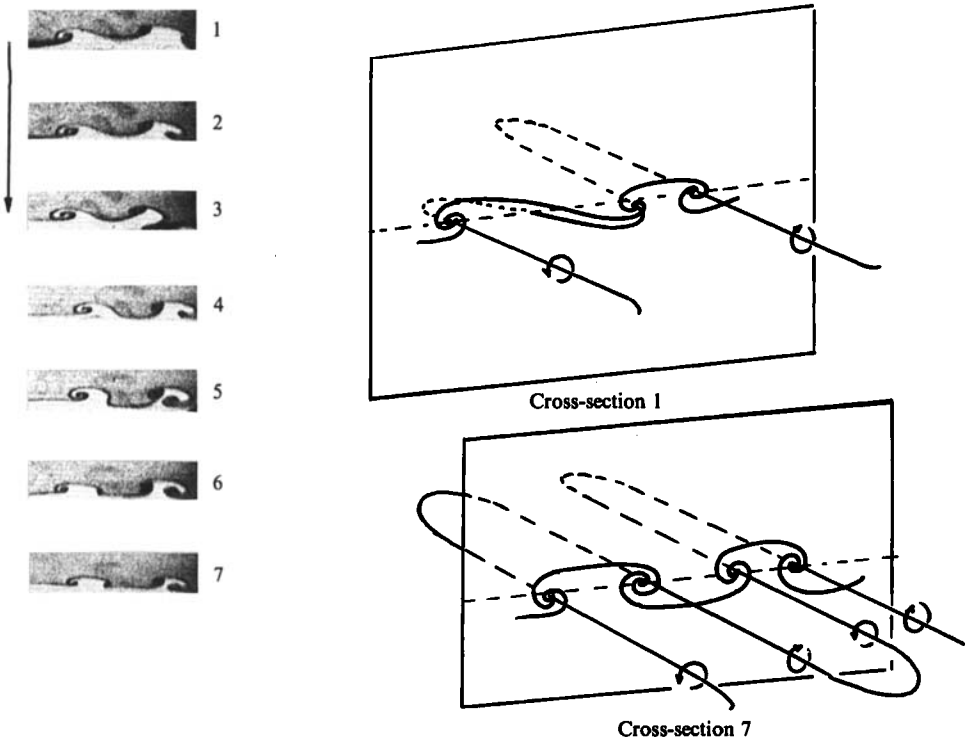

FIGURE 21. Vertical cross-cut pictures using LIF showing streamwise vortices developing into the 'stable configuration', i.e. counter-rotating pairs of streamwise vortices.

ular, the calculations presented in their figure 6 show a pattern remarkably similar to the one observed in our experiments.

Figure 20 sketches the development of such an instability in a region of positive strain rate on the interfacial surface. The vertical cross-cuts presented in this figure were obtained experimentally by moving the plane of illumination downstream with the convective velocity of the spanwise vortices. They show the development of the instability on the interface. Both this and all our other experimental observations are consistent with this proposed mechanism.

Figure 21 shows an explanation of an often-seen feature in the development of this instability. In frames 1–7, the formation of the streamwise vortices resulting from the above-described vortex stretching is shown. A schematic drawing is shown next to the frames. The frames were taken by moving the plane of illumination downstream with the convective velocity of the spanwise vortices. This case is particularly interesting since it shows the effect postulated in our 'axial-vorticity generating mechanism'. The so-called 'stable configuration' in this case has finally been achieved in frame 7. Here, the axial vorticity of the vortex second from the left has not been fully tilted and stretched so that its roll-up has not yet occurred (frames 1–4, cross-section 1). As stretching continues, however, (frames 5–7, cross-section 7) sufficient axial vorticity is produced to create a rolled-up interface. On other occasions, the same initial configuration (a pair of axial vortices of the same sign next to each other) was found to achieve the 'stable configuration', after undergoing a vortex pairing of the two dominant like-sign vortices.

The proposed mechanism to redistribute the spanwise vorticity in the axial direction does not require the full formation of two consecutive spanwise roll-ups. It simply requires the initiation of the formation of the first Kelvin–Helmholtz wave to produce positive strain (stretch) of the interface. In the cases where the perturbation is introduced in the layer at a location just prior to the first roll-up of the Kelvin–Helmholtz wave, we have observed a rapid development of the instability resulting in the formation of streamwise vortices even before we could observe the well-developed spanwise roll-up (see case 5, figure 10). Obviously, the magnitude of the strain existing in the region where the perturbation is introduced and the value of the spanwise vorticity which still exists at that location will determine the strength and scales of the resulting streamwise vortices.

4.4. *A three-dimensional reconstruction*

Streamwise vortical structures are convected downstream under the positive and negative strains created by the spanwise vortices. As they are being stretched and squeezed by the spanwise roll-ups, we have observed that they persist as recognizable coherent structures. The experimental results presented in figure 12 show that these streamwise vortices are present not only on the braids, but also inside the cores of the roll-ups. Analysis of the films reveal that the streamwise vortices are active flow structures inside the cores of the spanwise vortex, rather than fossil structures imported from the braids. Figure 22 is a three-dimensional reconstruction of the shear layer under investigation which was obtained from an analysis of high-speed cross-cut films using LIF. The schematic picture of the braids is essentially similar to the one postulated by Bernal (1981) and further refined by Jimenez *et al.* (1985). However, we are now able to reconstruct the cores and analyse the numerous interactions occurring among the streamwise vortices as they are being distorted by the spanwise ones.

As the crest of the spanwise vortex is rolling up, the counter-rotating pairs of

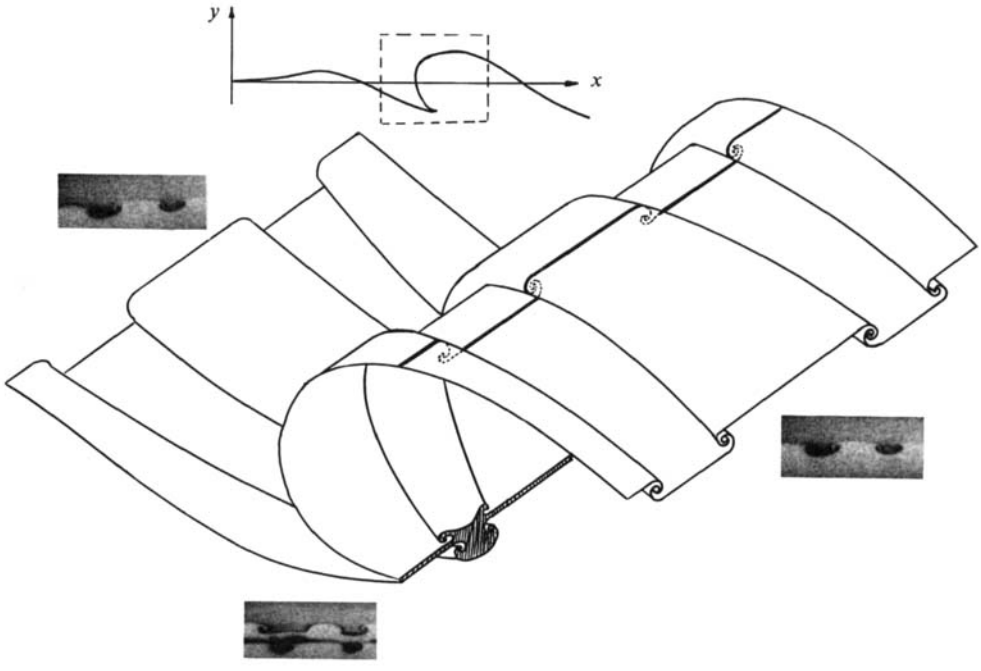

FIGURE 22. A three-dimensional reconstruction of the plane shear layer.

streamwise vortices along its inner and outer edge begin to interact with each other so that they become squeezed together at the tip of the roll-up by mutual interaction. Figure 23 summarizes some aspects of this interaction. Several cross-cut sections of a typical spanwise roll-up are presented showing how, as the crest of the spanwise wave rolls-up while moving upward, it breaks down under the effect of that interaction, thus producing smaller-scale vortices. This and other higher-order interactions will eventually result in a drastic increase of the interfacial area.

5. Summary and conclusions

An isothermal, plane shear layer between two reactive streams at different velocities was experimentally studied to investigate: (*a*) the origin of the streamwise vortical structures; (*b*) the nature and evolution of such streamwise vorticity and its interaction with the primary spanwise organized vortical structures, i.e. the precise location of their formation, scales, wavelength, etc; (*c*) the extent to which the streamwise vortical structures contributed to the entrainment and mixing in the free shear layer.

Both LIF and a DIV technique resulting from the reactive nature of the two flows were used to monitor the interface between the two mixing fluids while it was being stretched and corrugated under the influence of the different vortical structures.

The results corroborate the claim that the plane turbulent shear layer is composed of a secondary streamwise, coherent vortical structure which superimposes onto a primary spanwise one.

It was found that the plane shear layer is unstable to three-dimensional perturbations in the upstream conditions. This instability results in the formation of organized, three-dimensional streamwise vortical structures which propagate and

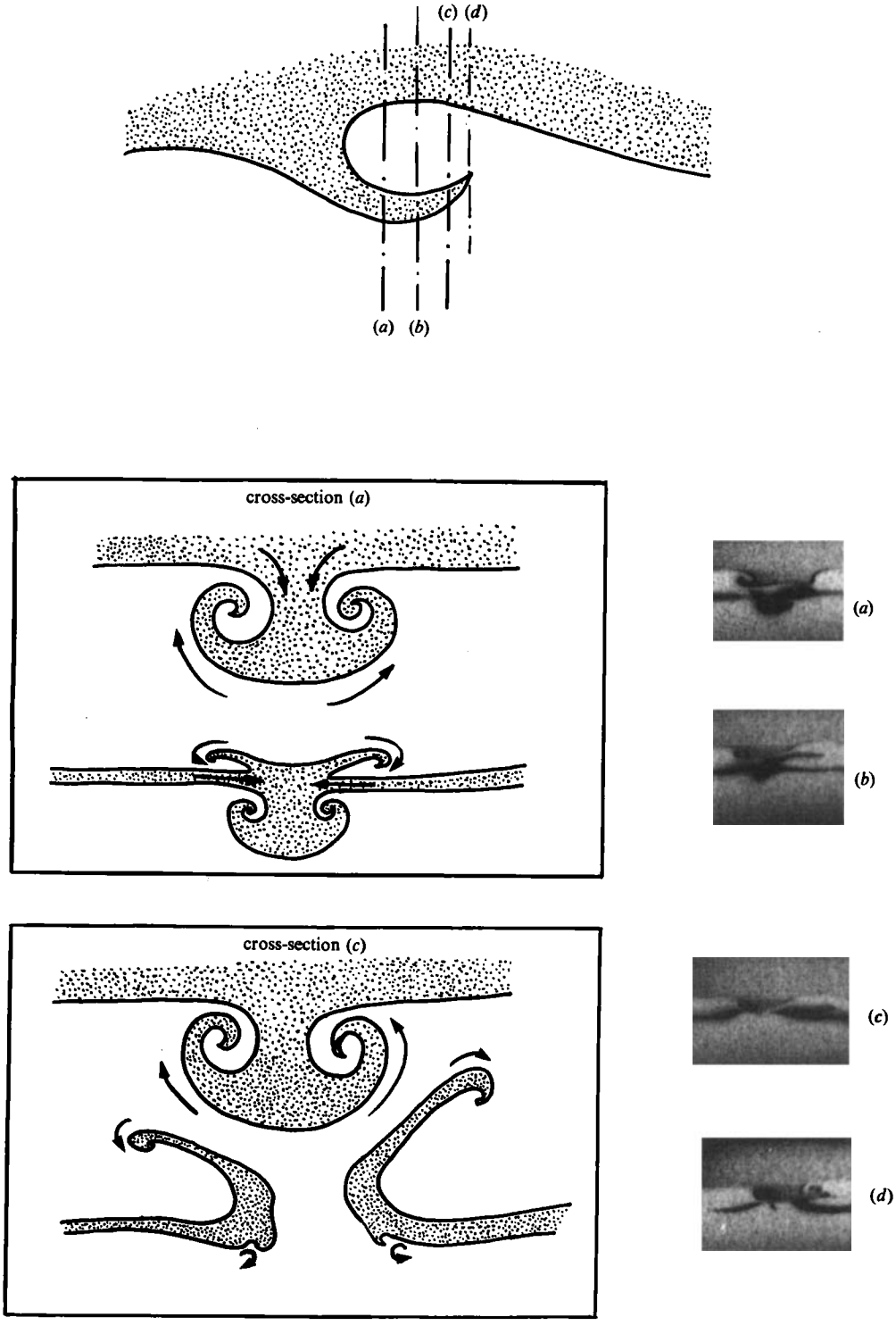

FIGURE 23. Details of the interaction between streamwise vortices situated on the inner and outer edge of the spanwise vortex core, showing the formation of smaller-scale eddies.

interact with each other under the positive and negative strain rates created by the spanwise vortices. Depending on the location and the intensity of the upstream disturbances, the position where the three-dimensional structures were first observed to form was found to change substantially.

Streamwise vortical structures were always observed first to form in the braids between the spanwise vortices and then to propagate into their cores.

For the cases analysed in this study, the three-dimensional streamwise vortical structures resulting from the secondary instability had a scale somewhat smaller than, but comparable with the spanwise structures, thereby contributing to a substantial part of the entrainment that occurred in the near region of the mixing layer.

The authors gratefully acknowledge the assistance received from Mr H. Choi during the acquisition of the photographic data. Discussions held with Professor Giles Corcos were very helpful in clarifying some of the points contained in this paper. His review and comments on the original manuscript are greatly appreciated. Special thanks are extended to Professor Frederick Browand who generously made his water-channel facility available to us (channel 2).

REFERENCES

Ashurst, W. T. & Meiburg, E. 1985 Three-dimensional shear layers via vortex dynamics. *11th Intl Assoc. of Mathematics and Computers in Simulation, Oslo, Norway.* Also, three-dimensional shear layers via vortex dynamics. *Saudia report*, SAND 85-8777.

Bernal, L. P. 1981 The coherent structure of turbulent mixing layers. Ph.D. dissertation, California Institute of Technology.

Bernal, L. P., Breidenthal, R., Brown, G. L., Konrad, J. H. & Roshko, A. 1981 On the development of three dimensional small scales in turbulent mixing layers. *Proc. 2nd Symp. Turbulent Shear Flows*, p. 305.

Breidenthal, R. 1978 A chemically reacting turbulent shear layer, Ph.D. dissertation, California Institute of Technology.

Breidenthal, R. 1980 Response of plane shear layers and wakes to strong three dimensional disturbances. *Phys. Fluids* **23**, 1929.

Breidenthal, R. 1981 Structure in turbulent mixing layers and wakes using a chemical reaction. *J. Fluid Mech.* **109**, 1.

Browand, F. K. & Troutt, T. R. 1980 A note on spanwise structure in the two-dimensional mixing layer, *J. Fluid Mech.* **97**, 771.

Browand, F. K. & Weidman, P. D. 1976 Large scales in the developing mixing layer. *J. Fluid Mech.* **76**, 127.

Brown, G. L. & Roshko, A. 1971 The effect of density difference on the turbulent mixing layer. *AGARD-CP*-93, 23-1–23-11.

Brown, G. L. & Roshko, A. 1974 On density effects and large structure in turbulent mixing layers. *J. Fluid Mech.* **64**, 775.

Corcos, G. M. 1979 The mixing layer: deterministic models of a turbulent flow. *U.C. Berkeley, Mech. Engng Rep.* FM-79-2.

Corcos, G. M. & Lin, S. J. 1984 The mixing layer: deterministic models of a turbulent flow. Part 2. The origin of the three-dimensional motion. *J. Fluid Mech.* **139**, 67.

Corcos, G. M. & Sherman, F. S. 1984 The mixing layer: deterministic models of a turbulent flow. Part 1. Introduction and the two-dimensional flow. *J. Fluid Mech.* **139**, 29.

Daily, J. W. & Lundquist, W. J. 1984 The three dimensional structure in a turbulent mixing layer. *20th Symp. (intl) on Combustion.* The Combustion Institute Ed.

Dewey, C. F. 1976 Qualitative and quantitative flow field visualization using laser induced fluorescence. *AGARD-CP*-193, 17-1–17-7.

DIMOTAKIS, P. & BROWN G. L. 1976 The mixing layer at high Reynolds number: large structure dynamics and entrainment. *J. Fluid Mech.* **78**, 535.

HAMA, F. R. 1963 Progressive deformation of a perturbed line vortex filament. *Phys. Fluids* **6**, 526.

HERNAN, M. A. & JIMENEZ, J. 1982 Computer analysis of a high speed film of the plane turbulent mixing layer. *J. Fluid Mech.* **119**, 323.

HO, C. M. & HUANG, L. S. 1982 Subharmonics and vortex merging in mixing layers. *J. Fluid Mech.* **119**, 443.

JIMENEZ, J. 1983 A spanwise structure in the shear layer. *J. Fluid Mech.* **132**, 319.

JIMENEZ, J. COGOLLOS, M. & BERNAL, L. P. 1985. A perspective view of the plane mixing layer. *J. Fluid Mech.* **152**, 125.

JIMENEZ, J., MARTINEZ-VAL, R. & REBOLLO, M. 1979 On the origin and evolution of three dimensional effects in the mixing layer. *Internal Rep.* DA-ERO 79-G-079, Universidad Politecnica de Madrid, Spain. Also, Rodrigo Martinez-Val. Tesis Doctoral E.T.S. de Ingenieros Aeronauticos. Universidad Politecnica de Madrid, Spain.

KONRAD, J. H. 1976 An experimental investigation of mixing in two dimensional turbulent shear flows with applications to diffusion limited chemical reactions. *Tech. Rep.* CIT-8-PU.

KOOCHESFAHNI, M. M. 1984 Experiments on turbulent mixing and chemical reactions in a liquid mixing layer. Ph.D. thesis, California Institute of Technology.

LASHERAS. J. C. & MAXWORTHY, T. 1985 Structure of the vorticity field in a plane, shear layer. *5th Symp. on Turbulent Shear Flows, 5–9 Aug., Cornell University, New York.*

LASHERAS, J. C. & CHOI, H. 1986 Stability of a plane turbulent shear layer to axial perturbations. *J. Fluid Mech.* (in preparation).

LIN, S. J. & CORCOS, G. M. 1984 The mixing layer: deterministic models of a turbulent flow. Part 3. The effect of plane strain on the dynamics of streamwise vortices. *J. Fluid Mech.* **141**, 139.

MASUTANI, S. M. & BOWMAN, C. T. 1984 The structure of a chemically reacting plane mixing layer. *Western States Sect./The Comb. Inst. Paper 84–44, 2–3 Apr. 1984, Boulder, Colorado.*

NEU, J. C. 1984 The dynamics of stretched vortices. *J. Fluid Mech.* **143**, 253.

OGUCHI, H. & INOUE, O. 1984 Mixing layer produced by a screen and its dependence on initial conditions. *J. Fluid Mech.* **142**, 217.

PIERREHUMBERT, R. T. & WIDNALL, S. E. 1982 The two- and three-dimensional instabilities of a spatially periodic shear layer. *J. Fluid Mech.* **114**, 59.

REBOLLO, M. 1973 Analytical and experimental investigation of a turbulent mixing layer of different gases in a pressure gradient. Ph.D. thesis, California Institute of Technology.

ROSHKO, A. 1980 The plane mixing layer flow visualization results and three-dimensional effects. *Proc. Intl Conf. on the Role of Coherent Structures in Modelling Turbulence and Mixing* (ed. J. Jimenez). Lecture Notes in Physics, vol. 136. Springer.

SEDNEY, R. 1973 A survey of the effects of small protuberances on boundary-layer flows. *AIAA J.* vol. II, no. 6.

TAN-ATICHAT, J. 1980 Effects of axisymmetric contractions on turbulence of various scales. Ph.D. dissertation, Mechanical and Aerospace Engineering, Illinois Institute of Technology.

WINANT, C. D. & BROWAND, F. K. 1974 Vortex pairing: the dynamics of turbulent mixing layer growth at moderate Reynolds number. *J. Fluid Mech.* **63**, 237.

WYGNANSKI, I., OSTER, D., FIEDLER, H. & DZIOMBA, B. 1979 On the perseverance of a quasi-two-dimensional eddy-structure in a turbulent mixing layer. *J. Fluid Mech.* **93**, 325.